9-18-2019

Atomically resolved domain boundary structure in lead zirconate-based antiferroelectrics

Tao Ma
Ames Laboratory

Zhongming Fan
Iowa State University, zfanad@iastate.edu

Xiaoli Tan
Iowa State University, xtan@iastate.edu

Lin Zhou
Iowa State University and Ames Laboratory, linzhou@ameslab.gov

Atomically resolved domain boundary structure in lead zirconate-based antiferroelectrics

Abstract

Domain boundary (DB) structures are of great importance for understanding the structure-property relationship in many ferroic crystals. Here, we present atomically resolved DB configurations in $PbZrO_3$-based antiferroelectric ceramics. The Pb-cation displacement relative to B-site cations is precisely determined using aberration-corrected scanning transmission electron microscopy. We find that 90° DBs in undoped $PbZrO_3$ can be as thin as one primitive cell of the perovskite structure, often appearing curved or zigzagged due to the complex dipole arrangement. In a chemically modified composition, $Pb_{0.99}Nb_{0.02}[(Zr_{0.57}Sn_{0.43})_{0.95}Ti_{0.05}]_{0.98}O_3$, in which incommensurate modulations are present, the DB has a typical thickness of at least two primitive cells, with more or less aligned dipole moments. Our findings provide insights into establishing the structure-property relationship in antiferroelectrics, shedding light on the design and fabrication of domain-boundary electronics.

Disciplines

Engineering Physics | Materials Science and Engineering

Comments

This article is published as Ma, Tao, Zhongming Fan, Xiaoli Tan, and Lin Zhou. "Atomically resolved domain boundary structure in lead zirconate-based antiferroelectrics." *Applied Physics Letters* 115, no. 12 (2019): 122902. DOI: 10.1063/1.5115039. Posted with permission.

Applied Physics Letters

Atomically resolved domain boundary structure in lead zirconate-based antiferroelectrics

Cite as: Appl. Phys. Lett. **115**, 122902 (2019); https://doi.org/10.1063/1.5115039
Submitted: 13 June 2019 . Accepted: 03 September 2019 . Published Online: 18 September 2019

Tao Ma, Zhongming Fan, Xiaoli Tan, and Lin Zhou

Applied Physics Letters ARTICLE scitation.org/journal/apl

Atomically resolved domain boundary structure in lead zirconate-based antiferroelectrics

Cite as: Appl. Phys. Lett. **115**, 122902 (2019); doi: 10.1063/1.5115039
Submitted: 13 June 2019 · Accepted: 3 September 2019 ·
Published Online: 18 September 2019

Tao Ma,[1] Zhongming Fan,[2] Xiaoli Tan,[2] and Lin Zhou[1,2,a)]

AFFILIATIONS

[1]Ames Laboratory, U.S. Department of Energy, Ames, Iowa 50011, USA
[2]Department of Materials Science and Engineering, Iowa State University, Ames, Iowa 50011, USA

[a)]Electronic mail: linzhou@ameslab.gov

ABSTRACT

Domain boundary (DB) structures are of great importance for understanding the structure-property relationship in many ferroic crystals. Here, we present atomically resolved DB configurations in $PbZrO_3$-based antiferroelectric ceramics. The Pb-cation displacement relative to B-site cations is precisely determined using aberration-corrected scanning transmission electron microscopy. We find that 90° DBs in undoped $PbZrO_3$ can be as thin as one primitive cell of the perovskite structure, often appearing curved or zigzagged due to the complex dipole arrangement. In a chemically modified composition, $Pb_{0.99}Nb_{0.02}[(Zr_{0.57}Sn_{0.43})_{0.95}Ti_{0.05}]_{0.98}O_3$, in which incommensurate modulations are present, the DB has a typical thickness of at least two primitive cells, with more or less aligned dipole moments. Our findings provide insights into establishing the structure-property relationship in antiferroelectrics, shedding light on the design and fabrication of domain-boundary electronics.

Domain boundary (DB) engineering is an emerging field in developing multifunctional ferroic materials, given that various domains and their boundary structures can lead to unique physical, magnetic, and electronic properties.[1–3] DBs that break the existing symmetry in the local area alter both the electrostatic potential and the electronic structure, often resulting in boundary superconductivity[4,5] or resistivity.[6] The morphology of DBs influences domain switching dynamics by either facilitating nucleation[7] or impeding domain wall motion.[8] Defect–DB interactions can cause domain boundary pinning by accumulated defect clusters, leading to electric fatigue or aging degradation.[9,10] It has been well documented that DBs can be created,[11,12] manipulated,[13–15] and annihilated,[16,17] opening opportunities for tailoring the desired properties of ferroic materials for next-generation domain-boundary electronics.

Precise DB engineering requires a deep understanding of boundary structures and the structure-property relationship. However, this knowledge is still elusive in many systems. For example, the $PbZrO_3$-based antiferroelectric (AFE) ceramics have been studied for over half a century[18,19] and considered as promising candidates for high energy-density capacitors,[20,21] electrocaloric devices,[22,23] and large-strain actuators.[24,25] While these functions are rooted in their unique domain and boundary structures, the dipole arrangement near the DB region remains obscure. Early studies on the AFE structure in $PbZrO_3$ revealed a fully compensated dipole moment in its unit-cell due primarily to antiparallel Pb-displacements.[19,26,27] Such an arrangement of dipoles forms stripes with a periodicity of four layers of its pseudocubic $\{110\}_c$ plane, known as the commensurate modulations (CMs) of $\frac{1}{4}\{110\}_c$. The modulations appear as a "twin-like" structure across the 60° or 90° DBs, and the dipoles are assumed to maintain a head-to-tail arrangement across the boundary.[28] When Sn and Ti, in conjunction with a small amount of Nb or La, are incorporated, the chemically modified ceramics transform to incommensurate phases of $\frac{1}{n}\{110\}_c$, (n is a noninteger between 6 and 8).[29–32] Transmission electron microscopy (TEM) studies have revealed that incommensurate modulations (ICMs) in the modified compositions have a variable thickness ~2 nm, corresponding to $n{\cdot}d_{\{110\}c}$, where $d_{\{110\}c}$ is the plane spacing.[30] The boundary structure in these modified ceramics with ICMs was previously assumed to be similar to that in $PbZrO_3$.[30–33] In our recent report,[34] we systematically investigated the dipole arrangement in a series of chemically modified $PbZrO_3$-based AFEs, and discovered that the dipole arrangement was, however, quite different from that in $PbZrO_3$: instead of the fully compensated antiparallel dipoles, "imbalanced antiparallel" or "orthogonal" arrangements were often observed, resulting in a net polarization in the "quasi-AFE" domains. In this letter, we present the atomically resolved DB structures in $PbZrO_3$ and a modified composition, $Pb_{0.99}Nb_{0.02}[(Zr_{0.57}Sn_{0.43})_{0.95}Ti_{0.05}]_{0.98}O_3$ (referred to as PZ-5 hereafter)

using aberration-corrected scanning transmission electron microscopy (STEM), and directly map out the Pb-cation displacement relative to the B-site cations. We demonstrate that in $PbZrO_3$, a 90° DB does not always lie on a straight $\{100\}_c$ plane, but usually becomes curved or zigzagged with either $\{110\}_c$ DB segments or planar defects inside the associated domains. In PZ-5 where ICMs are present, the 90° DB is, in fact, an atomically thin layer with aligned dipoles which can be regarded as a ferroelectric layer. Our findings will provide guidance for precise DB engineering, paving the way for the development of next-generation electronics.

$PbZrO_3$ and PZ-5 ceramics were prepared with the solid-state reaction method using PbO (≥99.9%), Nb_2O_5 (≥99.999%), ZrO_2 (≥99.99%), SnO_2 (≥99.997%), and TiO_2 (≥99.9%) as the starting materials. Detailed synthesis procedures were described in our previous reports.[31,34] For TEM observation, the ceramics were mechanically polished, followed by a short time, low-voltage Ar ion-milling to prepare electron-transparent specimens. High resolution high-angle annular dark-field (HAADF) images were captured using an FEI Titan Themis 300 probe-corrected STEM operating at 200 kV. The orientation of the observed grains was carefully aligned to the pseudocubic $[001]_c$ zone-axis by monitoring the Ronchigram. To minimize the beam-specimen interaction, scanning distortion, and readout noise, 40 images were recorded from each area with a frame rate of 0.2 s, and then cross-correlated and summed to produce a drift-corrected frame-integrated image. The atomic displacement of Pb-cations was determined by comparing the actual positions of the Pb columns with the ideal center of their surrounding B-site cations (Zr, Sn, Ti, and Nb), using a home-designed Python code (powered by "Hyperspy"[35] and "Atomap"[36] packages).

Figure 1(a) shows a typical bright-field TEM image of 90° domains in $PbZrO_3$. The selected area electron diffraction (SAED) pattern taken from the boundary region is embedded as the inset, which displays two sets of $\frac{1}{4}\{110\}_c$ superlattice spots that are originated from the CMs in the two associated domains. It can be seen that the DB comprises a segment in the left along $(110)_c$ and a segment in the right along $(100)_c$. Pb-displacement vector maps together with the corresponding HAADF-STEM images taken from the yellow box on the $(100)_c$ segment and the red box on the $(110)_c$ segment of the DB are presented in Figs. 1(b) and 1(c), respectively. Clearly, the off-center displacement of Pb columns alternates between two opposing $\langle 110\rangle_c$ directions in every two $\{110\}_c$ planes—the typical CMs of $\frac{1}{4}\{110\}_c$. In terms of the DBs, only the $(100)_c$ DB [Fig. 1(b)] matches the "herringbone pattern" predicted by Tanaka *et al.*[28] and the dipoles due to Pb-displacements form the "head-to-tail" configuration. It should be noted that the head-to-tail configuration is energetically favored in order to minimize the depolarization energy on the DB. Nevertheless, the $(110)_c$ DB [Fig. 1(c)], in which one stripe in the top left domain intersects with every stripe in the bottom right domain, has seldom been considered previously because the dipoles in two domains do not form the head-to-tail configuration. As can be seen in Fig. 1(c), there is no depolarization energy from the top left domain since all the dipoles are in-plane with the DB. Meanwhile, the depolarization energy from the bottom right domain is negligible since the dipoles reverse their directions every two $\{110\}_c$ atomic planes.[37] Consequently, the energy of such a $\{110\}_c$ DB in AFE crystals is minimized by a mechanism other than the traditional head-to-tail configuration.

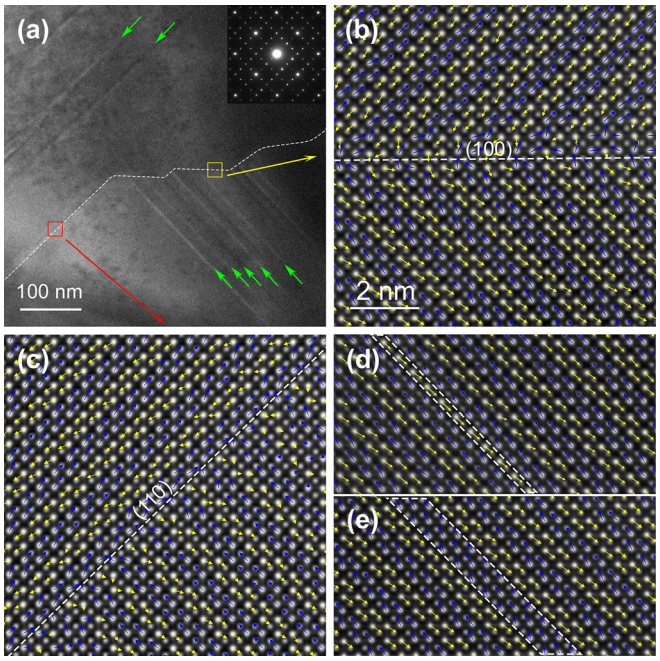

FIG. 1. (a) Typical bright-field TEM image of 90° domains in $PbZrO_3$ with line contrast. The corresponding SAED is shown in the inset. The dashed line highlights the DB. The green arrows mark the APBs that appear as thin lines in diffraction-contrast images. (b) and (c) Pb-displacement vector maps overlaid on atomic resolution HAADF-STEM images taken from the yellow and red boxes in (a), showing the $\{100\}_c$-type (b) and $\{110\}_c$-type (c) DB, respectively. (d) and (e) Two types of APBs with 1-layer (d) and 3-layer stripes (e), revealed by the Pb-displacement vector maps taken from the line area in (a).

AFE DBs could become more complicated than the segmented one if planar defects in the domains extend to the DB. In $PbZrO_3$, antiphase boundaries (APBs) are common planar defects and appear as thin lines in bright-field images [marked by the green arrows in Fig. 1(a)]. Two types of APBs were revealed from the Pb-displacement vector maps. As shown in Figs. 1(d) and 1(e), respectively, the APBs manifest as 1-layer and 3-layer stripes (highlighted by the dashed boxes). Note that these two types of APBs, both with a local polarization, are among the polar translation boundaries predicted theoretically by Wei *et al.*[12,38] However, those frequently observed in their $PbZrO_3$ film were not found here. Indeed, the internal strains of the 1-layer and 3-layer APBs are among the lowest of all the possible types according to their theoretical calculations.[12] It can be inferred that the formation energies of these APBs are also at the lower side. Therefore, they are the most common APBs observed in our bulk $PbZrO_3$ that had been sintered at a high temperature (1250 °C).

With these APBs, AFE DBs can exhibit a "zig-zag" shape. An example in another 90° DB in $PbZrO_3$ is illustrated in Fig. 2. In a normal segmented DB [Fig. 2(a)], the stripes in the upper and lower domains are all matched across the straight $(100)_c$ segments, even though there is a jog of a $(110)_c$ segment in the middle. Apparently, this "all-matched" configuration of the stripes across the $\{100\}_c$ boundary is preserved as long as no APBs reach the DB. However, this geometry is interrupted when an APB is present. As shown in Fig. 2(b), the stripes are no longer aligned after the insertion of a 1-layer APB. To

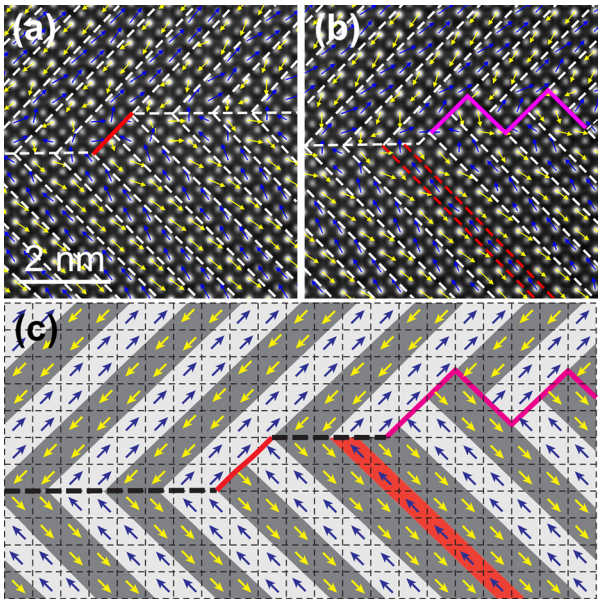

FIG. 2. (a) and (b) Domain configurations in $PbZrO_3$ revealed by the Pb-displacement vector maps. When APBs are not present, the stripes of CMs are all matched across the 90° DB even if a jog of a $(110)_c$ segment [red line in (a)] is inserted; the existence of an APB leads to a zigzagged DB [magenta lines in (b)]. (c) Schematic demonstrating both the all-matched and zigzagged domain configurations in $PbZrO_3$. The thin dashed lines outline the pseudocubic unit cells and the thick dashed lines indicate the straight DB with $\{100\}_c$ segments. The jog and zigzagged DBs are marked by the red and magenta dashed lines, respectively.

accommodate the 1-layer shift caused by the APB, the boundary is turned to a zig-zag shape with multiple $\{110\}_c$ segments, which gives rise to local depolarization energy. A schematic illustrating the domain configuration in $PbZrO_3$ is shown in Fig. 2(c).

It is well known that the thickness of DBs in ferroic materials varies from a few unit cells in ferroelectrics to tens of nanometers in ferromagnets.[39] In the undoped $PbZrO_3$ above, the dipoles change directions abruptly across a DB, giving a DB thickness of one primitive unit cell.

In the modified composition PZ-5, ICMs are the dominant microstructural feature. The atomic structures of DBs in AFE crystals with ICMs have not yet been reported previously. A typical bright-field TEM image of the 90° domains with a curved DB in PZ-5 is presented in Fig. 3(a) (highlighted with the dashed line). The ICMs inside the domains were confirmed by the textured contrast and the appearance of two sets of satellite spots in the SAED taken from the boundary region [inset in Fig. 3(a)]. A Pb-displacement vector map was taken from the boundary region marked by the box, as shown in Fig. 3(b). It can be seen that the Pb displacements in the lower domain are in the imbalanced antiparallel arrangement (those in blue have a larger magnitude than those in yellow), whereas the upper domain features the orthogonal arrangement of the Pb displacements, which tend to trace along the two orthogonal $\{100\}_c$ directions. Such a quasi-AFE state has been analyzed in detail in our recent work.[34] Between the two domains, the $(110)_c$ and $(100)_c$ DB segments can be clearly identified. It should be noted that ICMs are stochastic in thickness; structurally, they can be equivalently viewed as CMs plus random and aperiodic APB-like translational boundaries (as those observed in $PbZrO_3$).

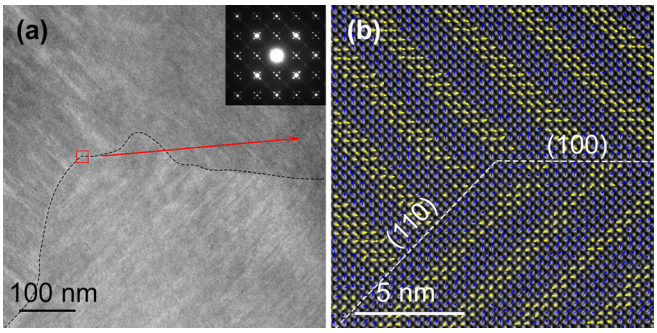

FIG. 3. (a) Typical bright-field TEM image of 90° domains in PZ-5 with a textured contrast. The corresponding SAED is shown in the inset. (b) Pb-displacement vector map overlaid on an atomic resolution HAADF-STEM image taken from the red box in (a), showing the $\{100\}_c$ and $\{110\}_c$ segments in the DB.

Therefore, the stripes across the boundary are always mismatched for a $(100)_c$ DB [consider the case in $PbZrO_3$ shown in Fig. 2(b)], giving rise to an uncompensated depolarization field along the entire $(100)_c$ DB segment. Such a depolarization field realigned the dipoles near the DB. Consequently, the material was found to develop a thin ferroelectric-like layer at the DB [marked by the white dashed box in Fig. 4(a)], in which the Pb displacements all roughly point upward [schematically illustrated in Fig. 4(b)]. For the $(110)_c$ DB segment, although the dipoles in the "imbalance antiparallel" domain remain in-plane with the DB, the stripes with stochastic thickness in the orthogonal domain also lead to a depolarization field along the entire $(110)_c$ segment. It should be noted that antiferroelectric crystals are also ferroelastic and internal elastic stresses may influence the domain boundary configurations. The present work is primarily on the Pb-cation displacement. Elastic stresses do not sense the direction of cation displacements. Consequently, the electrostatic energy presumably plays a predominant role in dictating the Pb-cation displacement in the vicinity of 90° antiferroelectric domain boundaries. Due to the randomness in the thickness of dipole stripes and the presence of uncompensated polarization in the ICMs, the thickness of the DB in the incommensurate AFE phase is at least 2 primitive cells, thicker than that in undoped $PbZrO_3$.

The atomic structures of the DBs revealed in the present work may play an essential role in dictating the properties, including the critical phase transition field E_F, of these $PbZrO_3$-based AFE

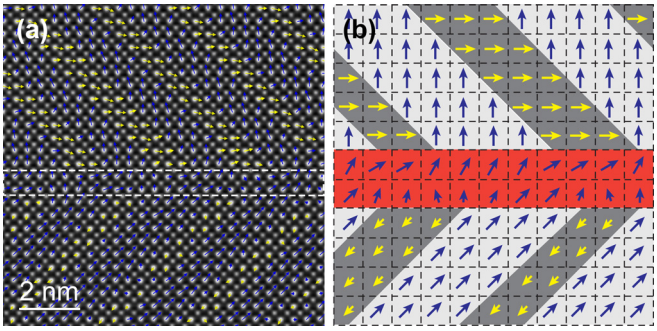

FIG. 4. Development of an atomically thin ferroelectriclike layer at the DB in PZ-5, as can be seen from (a) direct observation and (b) schematic illustration.

compositions. E_F is greater than 200 kV/cm at room temperature in undoped $PbZrO_3$,[32,40] while decreases to around 50 kV/cm in PZ-5.[34] Such a significant reduction in E_F is possibly related to the unique DB structures in two aspects. First, the formation of the ferroelectric phase out of the antiferroelectric matrix must undergo nucleation followed by a growth process.[41] In PZ-5, the nucleation process could be skipped due to the existence of a thin ferroelectric layer at DBs. As a result, the phase transition can easily take place via the fast expansion of the DB regions at the cost of AFE domains. Second, the applied electric field could initially reorient the dipoles within the thin ferroelectric layer at DBs, resulting in a much greater local depolarization field. We recently demonstrated that the interface between ferroelectric and antiferroelectric phases gains a good mobility once the uncompensated depolarization field emerges.[42] Subsequently, the global phase transition can be triggered at a lower applied field.

In summary, the complex DB structures in $PbZrO_3$-based AFEs were studied at the atomic scale using aberration-corrected STEM and Pb-displacement analysis. Basically, the curved 90° DBs in these ceramics are a combination of $\{100\}_c$ and $\{110\}_c$ boundary segments. In $PbZrO_3$, when an APB is present, a straight $\{100\}_c$ segment transforms to a zig-zag shape. In the modified composition, PZ-5, the dipoles near the DB are realigned by the local depolarization field, so that an atomically thin ferroelectriclike layer was observed at the DB. The thickness of DBs in $PbZrO_3$ can be as thin as one primitive cell, whereas that in PZ5 can be at least two primitive cells. Our findings reveal the atomically resolved DB structures in $PbZrO_3$-based AFE and will help establish the structure-property relationship in many boundary-induced phenomena in ferroic materials.

This work was supported by the National Science Foundation (NSF) through Grant No. DMR-1700014. All electron microscopy work was performed at the Sensitive Instrument Facility at Ames Laboratory, which is operated for the U.S. DOE by Iowa State University under Contract No. DE-AC02-07CH11358.

REFERENCES

[1]E. K. Salje, ChemPhysChem **11**, 940 (2010).
[2]D. D. Viehland and E. K. Salje, Adv. Phys. **63**, 267 (2014).
[3]G. Catalan, J. Seidel, R. Ramesh, and J. F. Scott, Rev. Mod. Phys. **84**, 119 (2012).
[4]J. Seidel, L. W. Martin, Q. He, Q. Zhan, Y. H. Chu, A. Rother, M. E. Hawkridge, P. Maksymovych, P. Yu, M. Gajek, N. Balke, S. V. Kalinin, S. Gemming, F. Wang, G. Catalan, J. F. Scott, N. A. Spaldin, J. Orenstein, and R. Ramesh, Nat. Mater. **8**, 229 (2009).
[5]W. Wu, Y. Horibe, N. Lee, S. W. Cheong, and J. R. Guest, Phys. Rev. Lett. **108**, 077203 (2012).
[6]T. Choi, Y. Horibe, H. T. Yi, Y. J. Choi, W. Wu, and S. W. Cheong, Nat. Mater. **9**, 253 (2010).
[7]C. T. Nelson, P. Gao, J. R. Jokisaari, C. Heikes, C. Adamo, A. Melville, S.-H. Baek, C. M. Folkman, B. Winchester, Y. Gu, Y. Liu, K. Zhang, E. Wang, J. Li, L.-Q. Chen, C.-B. Eom, D. G. Schlom, and X. Pan, Science **334**, 968 (2011).
[8]P. Gao, J. Britson, J. R. Jokisaari, C. T. Nelson, S. H. Baek, Y. Wang, C. B. Eom, L. Q. Chen, and X. Pan, Nat. Commun. **4**, 2791 (2013).
[9]Z. Fan and X. Tan, J. Eur. Ceram. Soc. **38**, 3472 (2018).
[10]Z. Fan, C. Zhou, X. Ren, and X. Tan, Appl. Phys. Lett. **111**, 252902 (2017).
[11]J. R. Whyte, R. G. McQuaid, P. Sharma, C. Canalias, J. F. Scott, A. Gruverman, and J. M. Gregg, Adv. Mater. **26**, 293 (2014).
[12]X. K. Wei, K. Vaideeswaran, C. S. Sandu, C.-L. Jia, and N. Setter, Adv. Mater. Interfaces **2**, 1500349 (2015).
[13]C. H. Ahn, T. Tybell, L. Antognazza, K. Char, R. H. Hammond, M. R. Beasley, Ø. Fischer, and J.-M. Triscone, Science **276**, 1100 (1997).
[14]L. J. McGilly, P. Yudin, L. Feigl, A. K. Tagantsev, and N. Setter, Nat. Nanotechnol. **10**, 145 (2015).
[15]J. R. Whyte and J. M. Gregg, Nat. Commun. **6**, 7361 (2015).
[16]S. Wada, S. E. Park, L. E. Cross, and T. R. Shrout, Ferroelectrics **221**, 147 (1999).
[17]H. Guo and X. Tan, Phys. Rev. B **91**, 144104 (2015).
[18]G. Shirane, E. Sawaguchi, and Y. Takagi, Phys. Rev. **84**, 476 (1951).
[19]E. Sawaguchi, H. Maniwa, and S. Hoshino, Phys. Rev. **83**, 1078 (1951).
[20]S. Kwon, W. Hackenberger, E. Alberta, E. Furman, and M. Lanagan, IEEE Electr. Insul. Mag. **27**, 43 (2011).
[21]B. Ma, Z. Hu, R. E. Koritala, T. H. Lee, S. E. Dorris, and U. Balachandran, J. Mater. Sci. **26**, 9279 (2015).
[22]P. D. Thacher, J. Appl. Phys. **39**, 1996 (1968).
[23]B. Peng, H. Fan, and Q. Zhang, Adv. Funct. Mater. **23**, 2987 (2013).
[24]X. Hao, J. Zhai, F. Shang, J. Zhou, and S. An, J. Appl. Phys. **107**, 116101 (2010).
[25]M. S. Mirshekarloo, K. Yao, and T. Sritharan, Appl. Phys. Lett. **97**, 142902 (2010).
[26]C. Kittel, Phys. Rev. **82**, 729 (1951).
[27]K. Yamasaki, Y. Soejima, and K. F. Fischer, Acta Crystallogr., Sect. B **54**, 524 (1998).
[28]M. Tanaka, R. Saito, and K. Tsuzuki, Jpn. J. Appl. Phys., Part 1 **21**, 291 (1982).
[29]Y.-J. Chang, J.-Y. Lian, and Y.-L. Wang, Appl. Phys. A **36**, 221 (1985).
[30]H. He and X. Tan, Phys. Rev. B **72**, 024102 (2005).
[31]H. He and X. Tan, J. Phys.: Consens. Matter **19**, 136003 (2007).
[32]X. Tan, C. Ma, J. Frederick, S. Beckman, and K. G. Webber, J. Am. Ceram. Soc. **94**, 4091 (2011).
[33]T. Asada and Y. Koyama, Phys. Rev. B **69**, 104108 (2004).
[34]T. Ma, Z. Fan, B. Xu, T.-H. Kim, L. Bellaiche, M. J. Kramer, X. Tan, and L. Zhou, "Uncompensated Polarization in Incommensurate Modulations of Perovskite Antiferroelectrics," Phys. Rev. Lett. (submitted).
[35]F. de la Peña, T. Ostasevicius, V. T. Fauske, P. Burdet, E. Prestat, P. Jokubauskas, M. Nord, M. Sarahan, K. E. MacArthur, D. N. Johnstone, J. Taillon, J. Caron, V. Migunov, A. Eljarrat, T. Furnival, S. Mazzucco, T. Aarholt, M. Walls, T. Slater, F. Winkler, B. Martineau, G. Donval, R. McLeod, E. R. Hoglund, I. Alxneit, I. Hjorth, T. Henninen, L. F. Zagonel, A. Garmannslund, and 5ht2, hyperspy/hyperspy: Hyperspy version 1.3.2, 2018.
[36]M. Nord, P. E. Vullum, I. MacLaren, T. Tybell, and R. Holmestad, Adv. Struct. Chem. Imaging **3**, 9 (2017).
[37]W. Y. Shih, W.-H. Shih, and I. A. Aksay, Phys. Rev. B **50**, 15575 (1994).
[38]X. K. Wei, C.-L. Jia, K. Roleder, and N. Setter, Mater. Res. Bull. **62**, 101 (2015).
[39]G. Catalan, J. F. Scott, A. Schilling, and J. M. Gregg, J. Phys.: Condens. Matter **19**, 022201 (2007).
[40]O. E. Fesenko, R. V. Kolsesova, and Y. G. Sindeyev, Ferroelectrics **20**, 177 (1978).
[41]Y. H. Shin, I. Grinburg, I. W. Chen, and A. M. Rappe, Nature **449**, 881 (2007).
[42]Z. Fan, F. Xue, T. Goknur, L.-Q. Chen, and X. Tan, Phys. Rev. Appl. **11**, 064050 (2019).